Journal of Alloys and Compounds 489 (2010) 233–236

Contents lists available at ScienceDirect

Journal of Alloys and Compounds

journal homepage: www.elsevier.com/locate/jallcom

Synthesis, characterization and electrical properties of the system $LaMn_xFe_{1-x}O_3$

P.P. Hankare[a,*], M.R. Kadam[a], P.D. Kamble[a], S.D. Jadhav[a], U.B. Sankpal[a], R.P. Patil[a], V.B. Helavi[a], N.S. Gajbhiye[b]

[a] Department of Chemistry, Shivaji University, Kolhapur -416004, MS, India
[b] Dr. Harisingh Gaur University, Sagar-470003, MP, India

ARTICLE INFO

Article history:
Received 15 July 2009
Received in revised form 6 September 2009
Accepted 10 September 2009
Available online 19 September 2009

Keywords:
Perovskite
X-ray diffraction
Thermal analysis
SEM
EDAX
Electrical properties

ABSTRACT

The system manganese substituted lanthanum ferrite viz. $LaMn_xFe_{1-x}O_3$ ($1.0 \leq x \geq 0$) was prepared by sol–gel autocombusion method. The structural characterization of the samples was carried out by X-ray diffraction technique and it is found that, the phase transfer from cubic to orthorhombic perovskite structure. The lattice parameter and crystallite size decrease with increasing Mn content. The phase formation of perovskite was revealed by thermal analysis technique. The surface morphology and elemental analysis of all the samples were carried out by scanning electron microscopy and energy dispersive X-ray spectroscopic technique, respectively. Electrical properties of the compounds show that, they exhibit semiconducting behavior. The substitution of manganese ions plays an important role in changing their structural, electrical and magnetic properties of lanthanum ferrite.

1. Introduction

The perovskites have very important structural, electrical and magnetic properties which are dependent on several factors such as, method of preparation, sintering temperature and time, chemical composition and substitution of various cations. The perovskite structure whose chemical composition is given by the general formula ABO_3 (A, rare earth metals and B, transition metals) has primitive cubic type of lattice [1,2]. Perovskites exhibit a variety of applications in electronics and magnetic materials [3]. At present, several chemical methods including ceramic, co-precipitation, sol–gel, and citrate precursor have been used to prepare perovskites [4–7].

In the present investigation, we focused on the synthesis of manganese substituted lanthanum ferrites powder was prepared by sol–gel autocombustion method. The aim of present work is to study the effect of manganese substitution of $LaFeO_3$ on structural, electrical properties of perovskites.

2. Experimental details

2.1. Synthesis technique

Crystalline powders of $LaMn_xFe_{1-x}O_3$ (where $x = 0.0, 0.2, 0.4, 0.6$ and 1.0) were prepared by sol–gel autocombustion method [8]. A.R. Grade anhydrous citric acid ($C_8H_8O_7$), manganese nitrate [$Mn(NO_3)_2{\cdot}4H_2O$] and ferric nitrate ($(FeNO_3)_3{\cdot}9H_2O$) were used as starting materials. The above nitrates were taken in appropriate proportions. An aqueous solution of citric acid was mixed with metal nitrate solutions and the few drops of concentrated HNO_3 were added to adjust the pH at 2. The mixed solution was kept on hot plate with continuous stirring at 70 °C. During the evaporation the solution becomes viscous and finally forms gel. The so formed gel was heated at 110 °C, when all remaining water was released from the mixture, the gel automatically burnt with glowing flints. The autocombustion was completed within a minute yielding the brown pulpy powders. The above powders were heated separately at 900 °C for 8 h to get final product. The granulated powders were pressed into pellets of 1.04 cm diameter under a pressure of 10 tonnes/cm^2 and thickness was adjusted to about 0.25 cm.

2.2. Characterizations

A computerised X-ray powder diffractometer (Philips PW-1710) with CuKα radiation (λ = 1.54056 Å) was used to identify the crystalline nature of the samples and to calculate lattice parameter and crystallite size. The lattice parameters were calculated for the cubic and tetragonal phase using following relations:

(a) For cubic phase $$\frac{1}{d^2} = h^2 + k^2 + \frac{l^2}{a^2} \quad (1)$$

(b) For orthorombic phase $$\frac{1}{d^2} = \frac{h^2}{a^2} + \frac{k^2}{b^2} + \frac{l^2}{c^2} \quad (2)$$

where a, b and c are lattice parameters, (hkl) is the Miller indices and d is the interplanar distance.

From the X-ray diffraction peaks, crystallite size was estimated using Debye Scherrer's formula [9]:

$$t = \frac{0.9\lambda}{\beta \cos\theta} \quad (3)$$

where symbols have their usual meaning.

The formation temperature of samples was checked by taking TGA/DTA curves on the SDT-2980 Ta instrument by heating the powders after autocombustion at a rate of 10 °C/min. from room temperature to 1000 °C in an air atmosphere. Scanning electron microscope (SEM) was used to study the morphology of the powders.

* Corresponding author. Tel.: +91 231 2609381.
E-mail address: p_hankarep@rediffmail.com (P.P. Hankare).

0925-8388/$ – see front matter © 2009 Elsevier B.V. All rights reserved.
doi:10.1016/j.jallcom.2009.09.059

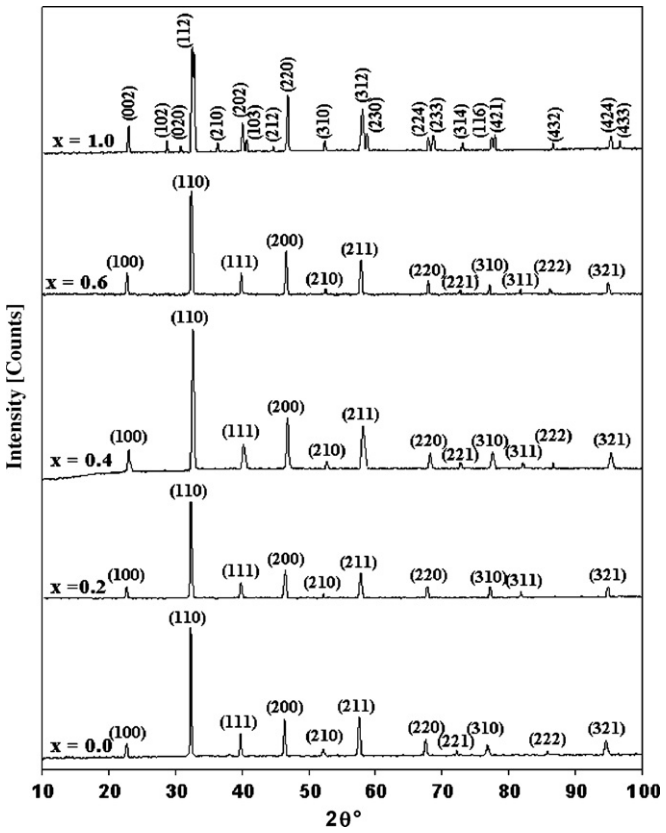

Fig. 1. XRD patterns of the system $LaMn_xFe_{1-x}O_3$.

The grain size of all the samples was calculated by Cottrell's method. An energy dispersive X-ray spectroscopy analyzer equipped with SEM was used for the compositional analysis. The electrical resistivity measurements in the temperature range 50–500 °C were made by two probe method. The electrical contacts were established by applying silver paste on both surfaces of the pellet. The graphs of the log ρ vs. 1000/T were plotted for all the samples under investigation and their energy of activation values (E) were calculated by using the equation:

$$E = 1.983 \times 10^{-4} \left[\frac{\log \rho}{1/T}\right] \text{eV}. \quad (4)$$

3. Results and discussion

3.1. X-ray diffraction study

The X-ray diffraction patterns of $LaMn_xFe_{1-x}O_3$ (where $x = 0.0$, 0.2, 0.4, 0.6 and 1.0) perovskite systems were shown in Fig. 1. XRD patterns of $x = 0.0$ to 0.6 compounds show formation of a single cubic phase perovskite structure, while $x = 1.0$ shows orthorhombic structure. The d_{hkl} and 2θ values were compared with the values reported in the literature (cubic, $LaFeO_3$, JCPDS File no. 75-0521) and (orthorhombic, $LaMnO_3$, JCPDS File no. 33-0713). Since the d_{hkl} values of the intermediate compositions are not reported in the literature, the values are compared with end compositions. In $LaFeO_3$, Fe^{3+} has high spin state t_{2g}^3 eg^2 configuration, therefore, distortion is not observed as all orbitals are filled bringing stability and therefore it was cubic. In $LaMnO_3$, Mn^{3+} in high spin state has t_{2g}^3 eg^1 electronic configuration and therefore it has no electron in $d_{X_2-Y_2}$ orbital and therefore lacks the spherical symmetry and brings distortion in lattice and therefore $LaMnO_3$ is orthorhombic. In perovskites Fe exists in two (2+ and 3+) oxidation states. To adjust this valency Mn acquires Mn^{4+} and Mn^{3+} oxidation states. At the octahedral site the average ionic radii of Mn ions is 0.595 Å [Mn^{3+} (0.65 Å) and Mn^{4+} (0.54 Å)] while that of the Fe ions is 0.715 Å [Fe^{3+} (0.65 Å) and Fe^{2+} (0.78 Å)] [10], thus lattice parameter decreases in the above system up to $x = 0.4$. Lattice parameter again increases in $x = 0.6$, it might be due to the phase transition from cubic to orthorhombic.

Table 1
Lattice constant and crystallite size of the system $LaMn_xFe_{1-x}O_3$.

Composition (x)	Lattice constant (Å)	Crystallite size (nm)
0.0	3.9260	27.95
0.2	3.9114	22.92
0.4	3.8856	16.97
0.6	3.9050	21.17
1.0	$a = 5.4516$ $b = 5.8068$ $c = 7.7538$	13.83

The sizes of the crystallites of the cubic and orthorhombic samples were evaluated by measuring FWHM and θ of the most intense peaks (1 1 0) and (1 1 2), respectively. The results are shown in Table 1. It is seen from the data that, the crystallite size decreases with increasing Mn content (except $x = 0.6$) [11].

3.2. Thermal analysis

Phase formation of perovskite oxide was investigated by the thermal analysis of powders after autocombustion was carried out from room temperature to 1000 °C in air atmosphere at the heating rate of 10 °C/min. The TGA–DTA curve for the sample is shown in Fig. 2. The TG curve shows that, the initial sample losses are about 46% weight of its original weight.

Initially, the 20% loss in weight was observed by removal of absorbed water and water of crystallization up to 200 °C. An exothermic peak at about 200 °C was observed due to evolution of heat by removal of absorbed water and water of crystallization. The decomposition of citrate complex was started at 250 °C and it was completed at 520 °C. During this decomposition, sample lost 28% weight [12,13]. The DTA curve shows exothermic peak at about 403 °C due to the formation of perovskite oxides.

3.3. Morphology and compositional analysis

The SEM micrographs of the system $LaMn_xFe_{1-x}O_3$ are shown in Fig. 3(a)–(e). This study reveals that, all the samples show fine grains. The average grain size of perovskite samples increases with manganese content. The average grain size was calculated by Cottrell's method [14]. The average grain size lies in the range 0.228–0.996 μm. From the micrograph, it is observed that the

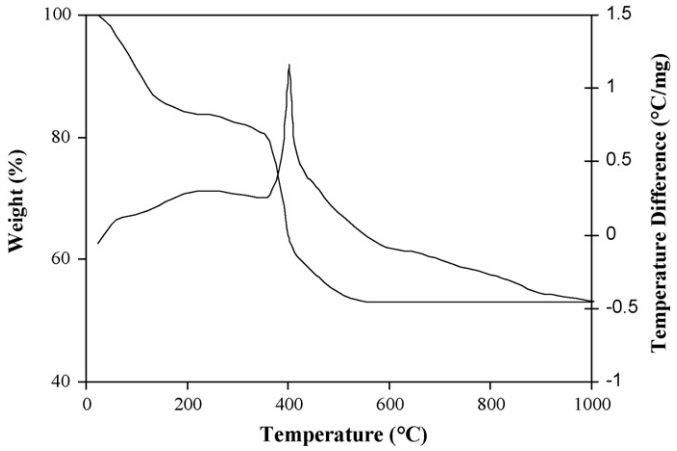

Fig. 2. TGA and DTA curves for $LaMnO_3$.

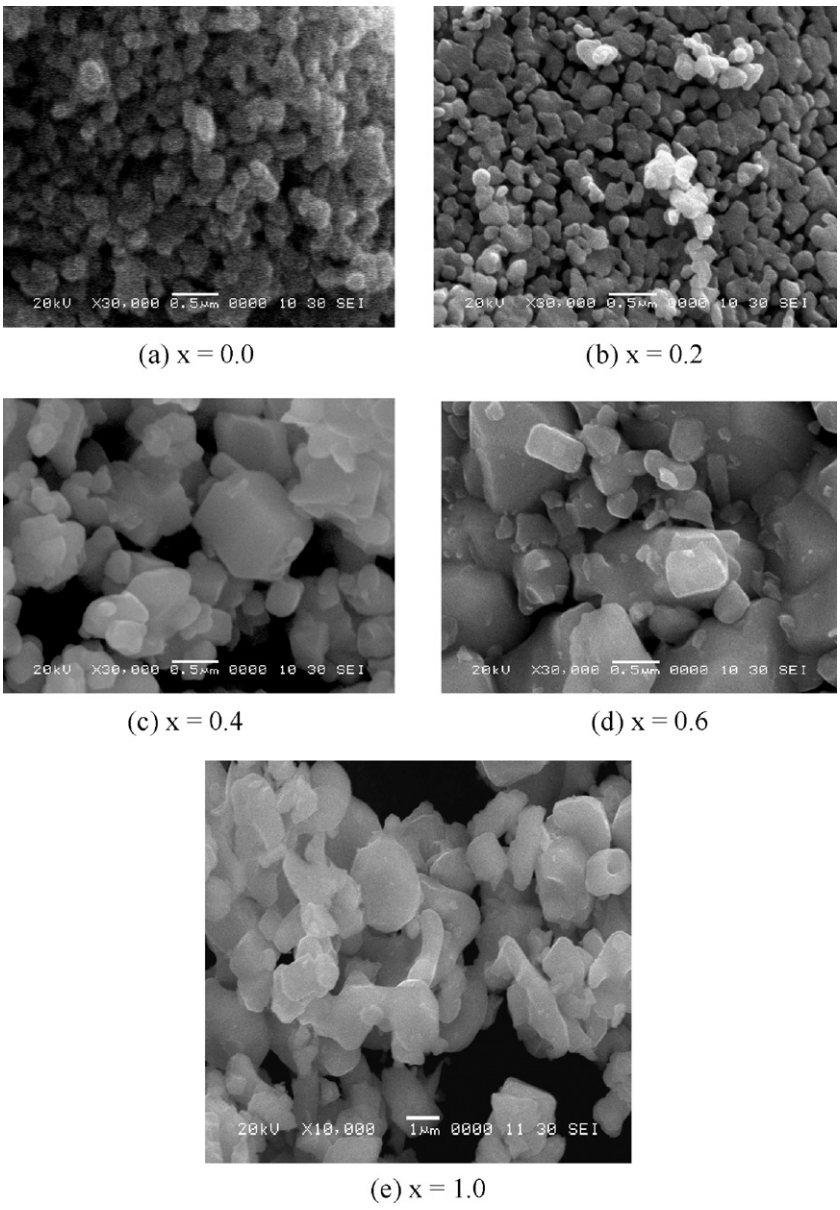

Fig. 3. SEM photographs of the system $LaMn_xFe_{1-x}O_3$. (a) $x = 0.0$, (b) $x = 0.2$, (c) $x = 0.4$, (d) $x = 0.6$ and (e) $x = 1.0$.

porosity decreases with increasing grain size due to the grain size reduces the grain boundary area.

The composition of the product has been determined by the EDAX spectra for the elemental analysis of $LaMnO_3$ sample is shown in Fig. 4. The spectra show the presence of La, Mn and O in the sample and did not contain any elemental impurities. This result indicates that, the cation impurities did not take part in the reaction. It is found that the atomic ratio of Mn:La of $LaMnO_3$ compound is 1:1.008 [15–17].

3.4. D.C. resistivity measurements

Fig. 5 shows the D.C. electrical resistivity of the samples with temperature. It is observed that, all samples show the semiconducting nature i.e. electrical resistivity decreases with increasing temperature. The D.C. resistivity of samples varies between 10^2 and 10^7 Ω cm. It also shows that the resistivity decreases from $x = 0.0$ to $x = 0.4$, increases for $x = 0.6$ and again decreases for $x = 1.0$, probably because both Mn and Fe have variable oxidation states. In tran-

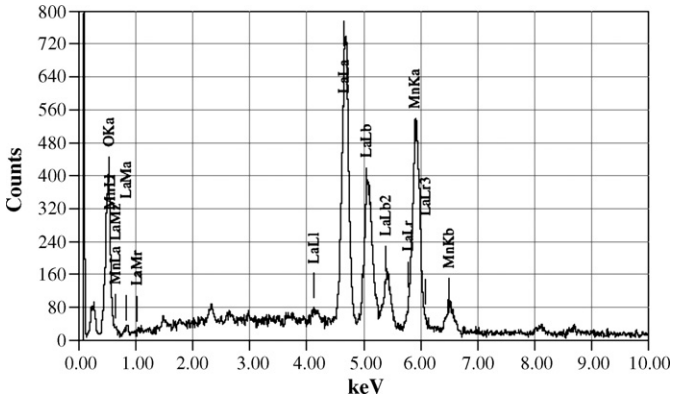

Fig. 4. EDAX pattern for the sample $LaMnO_3$.

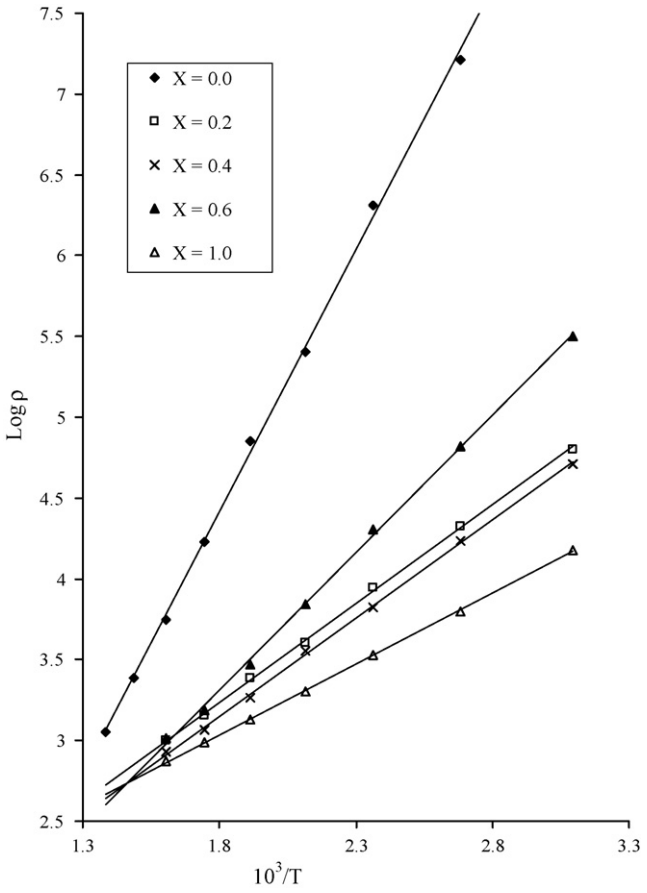

Fig. 5. Plots of log ρ vs. 1000/T of the system $LaMn_xFe_{1-x}O_3$.

sition metal oxides, it is observed that the electrical resistivity is low if the compound contains the cation of the same element situated at the similar site but with their valency differing by unity [18]. The activation energy varies in the range 0.174–0.642 eV and shows decreasing behavior with increasing Mn content [19]. The activation energy of $LaMnO_3$ is 0.174 eV, which is near about the reported value of Subba Rao et al. [20].

4. Conclusion

The pH controlled $LaMn_xFe_{1-x}O_3$ samples were synthesized by sol–gel autocombustion method. The crystal structures of $x = 0.0$ to $x = 0.6$ compounds were cubic perovskite, while $x = 1.0$ compound was orthorhombic. Experimental results revealed that, the lattice constant and crystallite size decrease with the increasing of Mn content (except $x = 0.6$). Thermal analysis shows the perovskites are formed at about 520 °C. Morphology and elemental analysis shows that, the average grain size lies in the range of 0.228–0.996 μm and metals in the samples are in their stoichiometric proportions as expected. Electrical resistivity plot shows that all the samples are semiconducting in nature.

Acknowledgement

One of the author (PPH) is thankful to U.G.C., New Delhi for sanctioning Major Research Project, F. No.32-289/2006 (SR).

References

[1] G.A. Geguzina, V.P. Sakhnenko, Crystallogr. Rep. 49 (2004) 15.
[2] G.P. Joshi, N.S. Saxena, R. Mangle, A. Mishra, T.P. Sharma, Bull. Mater. Sci. 26 (2003) 387.
[3] A.H. Robeck, Bell Syst. Technol. J. 46 (1967) 1901.
[4] N.P. Vyshatko, V. Kharton, A.L. Shaula, E.N. Naumovich, M.B. Marques, Mater. Res. Bull. 38 (2003) 185.
[5] P. Benedictita, V. Murugavel, Ponnambalam, A.R. Raju, Proc. Indian Acad. Sci. (Chem. Sci.) 115 (2003) 519.
[6] C. Sun, K. Sun, Physica B 391 (2007) 335.
[7] C.N.R. Rao, Om Parkash, P. Ganguly, J. Solid State Chem. 15 (1975) 186.
[8] M. Chen, X.-M. Zheny, Indian J. Chem. 41A (2002) 2277.
[9] A.T. Raghavender, D. Pajic, K. Zadro, T. Milekovic, P. Venkateshwar Rao, K.M. Jadhav, D. Ravinder, J. Mag. Mag. Mater. 316 (2007) 1.
[10] R.D. Shannon, C.T. Prewitt, Acta Crystallogr. B26 (1970) 1076.
[11] A.V. Salker, T. Vaz, Ind. J. Chem. 43A (2004) 710.
[12] E. Traversa, P. Nunziante, M. Sakamoto, Y. Sadaoka, R. Montanari, Mater. Res. Bull. 33 (1998) 673.
[13] N.S. Gajbhiye, G. Balaji, Thermochem. Acta 385 (2002) 143.
[14] A. Cottrell, An Introduction to Metallurgy, Edward Arnold, London, 1967.
[15] R. Vengadesh Kumara Mangalam, A. Sundaresan, J. Chem. Sci. 118 (2006) 99.
[16] H. Provendier, C. Petit, J.L. Schmitt, A. Kiennemann, J. Mater. Sci. 34 (1999) 4121.
[17] G. Gnanaprakash, J. Philip, B. Raj, Mater. Lett. 61 (2007) 4545.
[18] V. Edward, H. Bongio, F.C. Black, D. Raszewski, C. Edwards, J. Mcconville, V.R.W. Amarakoon, J. Electroceram. 14 (2005) 193.
[19] V.V. Kharton, A.P. Viskup, E.N. Naumovich, A.A. Tonoyan, O.P. Reut, Mater. Res. Bull. 33 (1998) 1087.
[20] G.V. Subba Rao, B.M. Wanklyn, C.N.R. Rao, J. Phys. Chem. Solids 32 (1971) 345.